

EXPERIMENTAL STUDY OF WATER MIST SUPPRESSION MECHANISMS IN A FORCED FLOW BOUNDARY LAYER FLAME

Chuka C. Ndubizu
Geo-Centers, Inc. at NRL

Ramagopal Ananth and Patricia A. Tatem
Naval Research Laboratory

ABSTRACT

This paper presents preliminary results of an experimental study of water mist suppression mechanisms in a PMMA boundary layer diffusion flame. It is motivated by the need to optimize the design of water mist systems for deployment in Navy ships. Results of tests to characterize the base case (no suppressant) flame and tests to study the effects of oxygen dilution are presented. These results can be summarized as follows:

- Temperature profiles in the gas phase show a higher gradient in the leading section, and this is consistent with the higher burning rate measured in this section.
- A disproportionately higher burning rate is measured in the leading section; therefore, most of the mist should be delivered in this section for optimum effectiveness.
- The dilution of oxygen tends to destabilize the flame by increasing the quenching distance. With 19.6% oxygen (by volume) the quenching distance was about 15 mm under the current test conditions. Oxygen dilution also led to lower flame temperature, which is due to the decrease in heat generation rate especially in the leading section of the flame where chemistry is important.

INTRODUCTION

Water mist has been adopted as the replacement fire fighting agent for Halon 1301 in machinery space in future US Navy ships. A better understanding of the role of various water mist fire suppression mechanisms is required to produce an optimized design of water mist systems for application in other ship spaces. Fundamental studies on water mist fire suppression mechanisms have been carried out in two main fire configurations: co-flow [1-4] and counter-flow [5,6]. Water mist is known to suppress fire by thermal cooling, oxygen dilution, and radiation attenuation. The thermal cooling effects result from the absorption of latent heat and sensible heat either in the gas phase or from the burning solid surface. Each gram of water absorbs about 3.7 KJ *tu* go from water at 20 °C to steam at 1500 °C. Upon evaporation, its volume increases 1600 times and the water vapor dilutes oxygen concentration in the gas mixture. The role of these suppression mechanisms in boundary layer diffusion flames has not been investigated even though boundary layer flames are prevalent in wall fires and wind-driven fires. Laboratory studies in boundary layer flames utilize 2-D diffusion flames over porous plate burners or non-charring solid fuels like **PMMA**. It is desirable to characterize a stable un-suppressed flame to begin with before conditions are changed to obtain suppression.

The objective of this paper is to present preliminary results of an experimental study of water mist suppression mechanisms in a boundary layer diffusion flame. Specifically, the paper will discuss the characterization of the base case (no suppressant) forced flow boundary layer flame over **PMMA**. Also the effects of diluting the oxygen concentration in the oxidizer air flow (with nitrogen) on the flame temperature, surface heat feedback, and burning rate will be presented.

EXPERIMENTAL

Figure 1 is a schematic of the experimental setup. It consists of the wind tunnel, the **PMMA** sample and the sample holder, an ATC weigh cell, and thermocouples mounted on a set of Velmex X-Y unislides. The wind tunnel has a 36 x 45 x 61 cm plenum at one end into which an Ametek RJ054[®] variable speed blower pumps air. In tests where the oxygen concentration is diluted below 21-mole%, a pre-determined flow of nitrogen is mixed with the air stream from the blower before it enters the plenum. Further mixing of the air and additional nitrogen takes place in the plenum and along the wind tunnel. Pressure built up in the plenum drives the flow of the oxidizer through the wind tunnel and hence the effects of the blower on the flow are minimized. The flow velocity in the wind tunnel is selected by adjusting the speed of the

blower. The tunnel is made of 3 mm (1/8 in.) thick steel and is air tight except at the end. The burning sample is positioned outside the tunnel, at the center of the tunnel exit. This makes it easier for the thermocouples to be moved freely in and out of the flame to measure the gas phase temperatures. In tests with water mist, this arrangement will prevent water other than that carried by the air (e.g., water dripping from the “ceiling” of the tunnel) from entering the flame. Any such drip of water cannot be accounted for and will taint the results. The holder is positioned with its leading edge against the tunnel exit. It has a leading plate section of 4 cm between the sample leading edge and the exit of the tunnel, a trailing section 5 cm beyond the sample trailing edge, and a 5 cm “wing” on both sides of the sample (insert, Figure 1). A thin strip of quartz is placed between the PMMA sample and the walls of the holder on all the four sides, which reduces the rate of heat transfer to the holder walls. The samples (7.7 x 9.5 cm) are made from a Cyro Acrylite GP® sheet nominally 2.54 cm (1 in.) thick. The sample and holder sit on an ATC weigh cell model 6005D, which continuously measures the combined weight of the sample and holder.

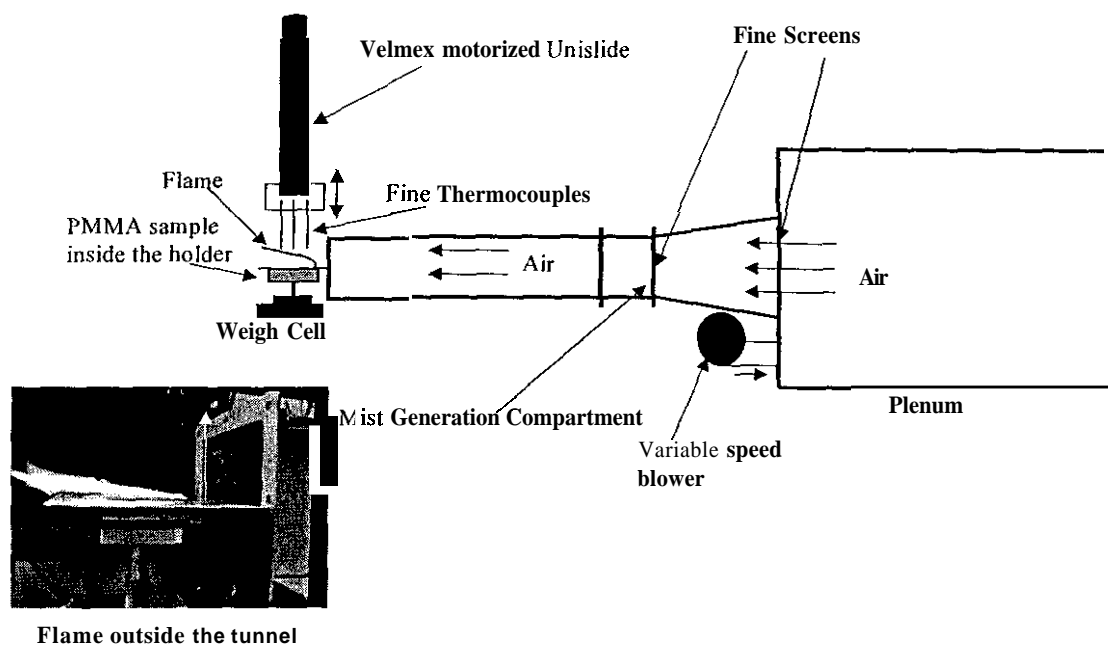


Figure 1. Schematic of the wind tunnel.

Five R-type thermocouples, 50 μm (0.002”) in diameter are mounted on the X-Y unislide arrangement such that they can be moved precisely up and down (Y- direction) across the flame thickness or left and right (X-direction) along the length of the flame. Voltage signal from the thermocouples goes through the National Instruments@TC 2095 terminal block into the SCXI 2000 chassis where the signals are conditioned and digitized. LabView software is used to precisely position the thermocouples as well as read the digitized signals and convert them to temperatures.

The velocity profile of the air is measured at the exit of the tunnel (measurement location) using a hot wire anemometer. This gives the centerline velocity of the in-coming airflow (U), as well as the velocity profile over the sample. It has been shown previously [7] that U does not decrease significantly within the measurement location. The sample surface is ignited by a uniform radiation from the radiant panel, and a stable 2-D flame is established over the sample in less than 15 sec. The radiant heat is turned off after ignition. Gas phase temperatures are mapped immediately a stable flame is established, and measurement is completed in less than 45 sec. This minimizes the effects of flame movement as the sample surface regresses. The sample is allowed to burn for a known length of time before the flame blow-out.

After the sample cools down, its thickness along the centerline is measured at various stream-wise locations from the leading edge, X , with a digital micrometer whose accuracy is ± 0.003 mm. The average

sample regression rate at each location is the difference in thickness, after correction for PMMA thermal expansion, divided by the test duration. At each location along the sample length, the fraction of the total mass burned up to that location is also determined using the measured regression rate, PMMA density, and sample width. The results are presented in the next section for base case test (21% oxygen) and for tests where the air was diluted with additional nitrogen to 20% oxygen and 19.6% oxygen.

RESULTS AND DISCUSSIONS

GAS PHASE TEMPERATURE

Figure 2 shows a typical temperature mapping of the boundary layer diffusion flame on a black PMMA sample at five X locations (10 mm, 21 mm, 37 mm, 58 mm, and 79 mm from the sample leading edge). The inlet velocity, U was 84 cm/sec. These data were measured within the first minute into the test and they have been corrected for thermocouple bead radiation. The measured peak temperature at a location increases stream-wise from the leading edge because of convection. A maximum of about 1902 ± 40 K is reached about 21 mm from the leading edge and thereafter the value of the peak temperature decreases as the plume zone is approached. The uncorrected value of the maximum flame temperature is 1835 ± 40 K. Holve and Sawyer [8] measured an uncorrected peak temperature of 1770K in a PMMA opposed flow diffusion flame using 75 μm diameter thermocouples. The temperature profiles show that the temperature gradients are higher in the leading section and decrease with X . This is consistent with the stream-wise decrease in heat feedback and burning rate discussed in the next section. In Figure 2, the original heights above the sample are distances between the sample surface and thermocouple bead before the flame was ignited and the surface began to regress. Therefore, the zero height in Figure 2 is not necessarily the sample molten surface at the time of the measurement. Because of surface regression, the thermocouples, especially the ones at the leading section, did not touch the molten surface during the measurement. However, the slope of the curves, of the thermocouples downstream near the zero height, shows that these thermocouple beads may have gotten into the molten layer. The last two thermocouples measured temperatures of about 649 to 644 K at zero height. Typical values for PMMA vaporization temperature reported in the literature range from 630 to 680 K [8, 9, 10].

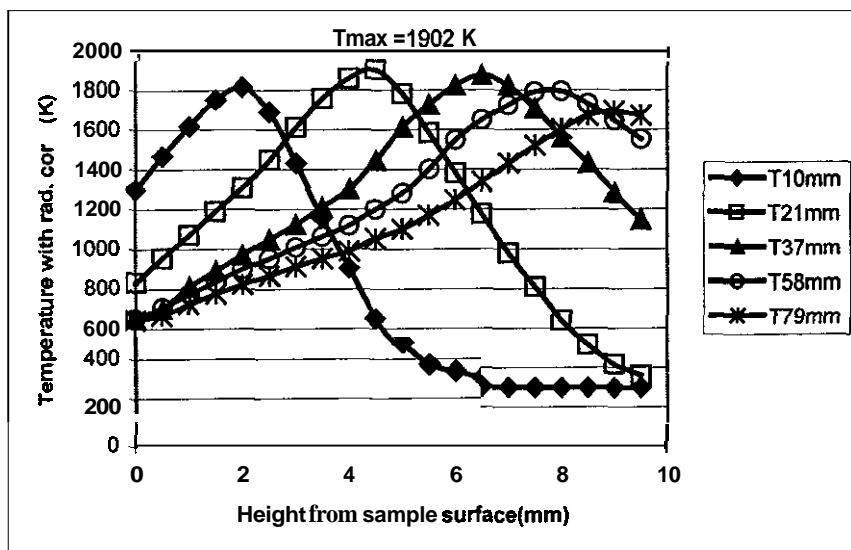


Figure 2. Gas phase temperature profiles for the base case test (21% O_2).

Similar trends are obtained in the temperature profiles in tests with additional nitrogen except for some differences, to be discussed with Figure 3, which shows the temperature profile with 19.6% oxygen concentration. With this oxygen dilution the flame was observed to attach about 15 mm downstream from

the leading edge instead of at the edge, as a result of the dilution effects. Hence, the first thermocouple at $X=10$ mm measured very low temperatures because it never got into the flame. Because of the quenching distance with oxygen dilution, the temperature profiles can only be compared with the corresponding ones in the base case ($X=15$ mm). The profile at $X=21$ mm in the base case flame could be compared with the profile at $X=37$ mm (approximately) in the flame with dilute oxygen. This comparison shows that the peak temperature decreased by about 150 K and flame standoff distance increased by about 1.0 mm when oxygen concentration dropped to 19.6%. Because of the decrease in oxygen concentration, the fuel had to diffuse to a higher distance to obtain a stoichiometric mixture. Since the temperature is lower and the flame standoff distance is high in the test with 19.6% oxygen, the heat feedback to the surface will be lower and the burning rate will be lower, as will be shown in the next section.

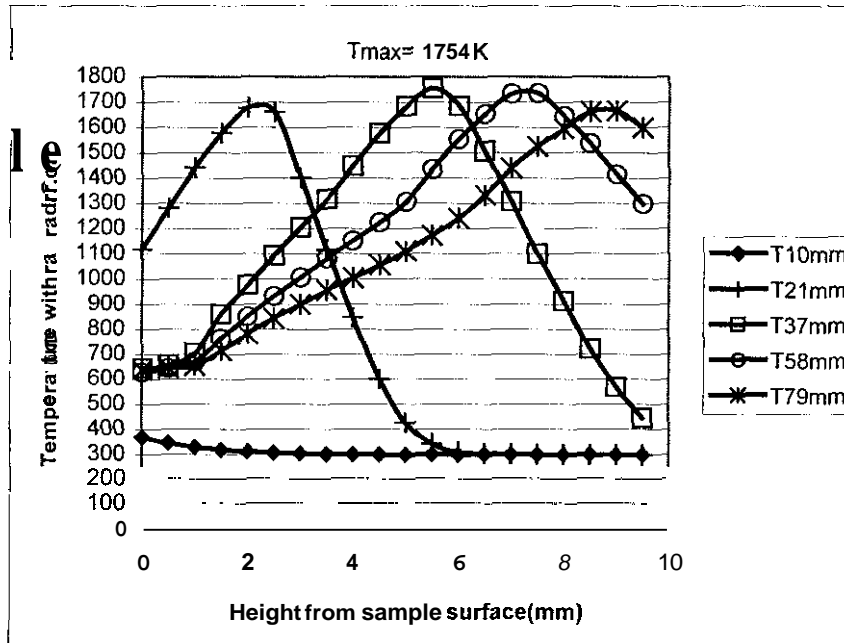


Figure 3. Gas phase temperature profiles for test with 19.6% O_2 .

SAMPLE BURNING RATE

Figure 4 shows the regression rate as a function of the stream-wise distance from the leading edge ($X=0$). The data represent the average regression rate (over the test duration) with normal air (21% O_2). Recently we have shown [7] that the sample burning rate decreases significantly with time especially in the leading section. However, all the results presented here are for test durations of 5 min. Several tests were repeated to show the scatter in the data. The surface regression rate drops sharply, streamwise along the sample length because of non-uniform heat feedback from the boundary layer flame. However, this drop in regression rate with X does not follow the $X^{-0.5}$ variation predicted by Emmon's classical theory [11] for flat plate boundary layer diffusion flame. A curve fit through the data shows that the variation is more like $X^{-0.8}$. This sharp drop in burning rate with X implies that a disproportionately higher percentage of the burning takes place in the leading section of the sample as will be discussed in the next section. Earlier workers [9] had measured a burning rate, which is almost constant with X and not varying as $X^{-0.5}$. They attributed the discrepancy to solid phase unsteadiness and sample surface re-radiation effects.

Figure 5 compares the sample burning rate for the base case tests with those for tests with 20 and 19.6% oxygen concentrations, and it shows the effects of oxygen dilution on the sample burning rate. In all three tests, the regression rate decreases sharply with distance from the leading edge. The base case peak regression rate of 0.92 mm/min occurred 3 mm from the leading edge. With 20% O_2 , peak regression rate is about 0.77 mm/min at $X = 5$ mm; with 19.6% O_2 , it is about 0.56 mm/min at $X = 18$ mm. Figure 5 shows that virtually no burning took place in the first 10 mm of the sample in the test with 19.6% O_2 .

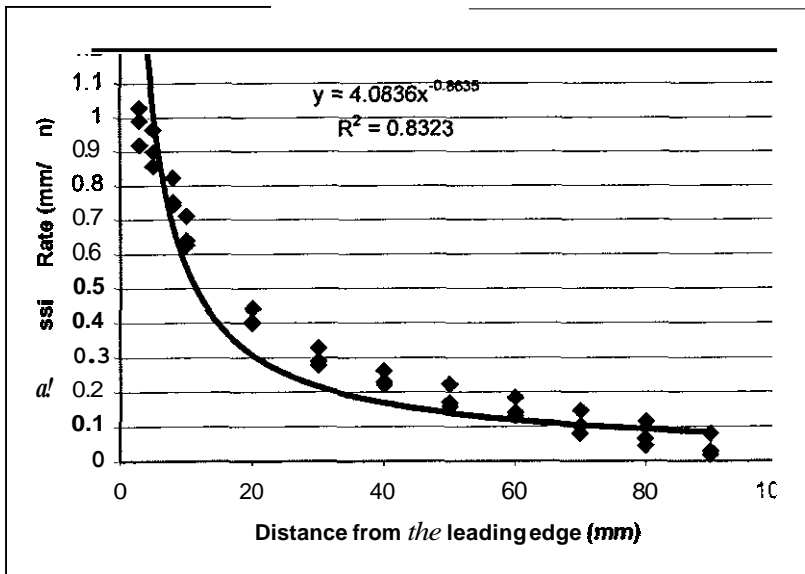


Figure 4. Variation of burning rate with stream-wise distance for the base case test.

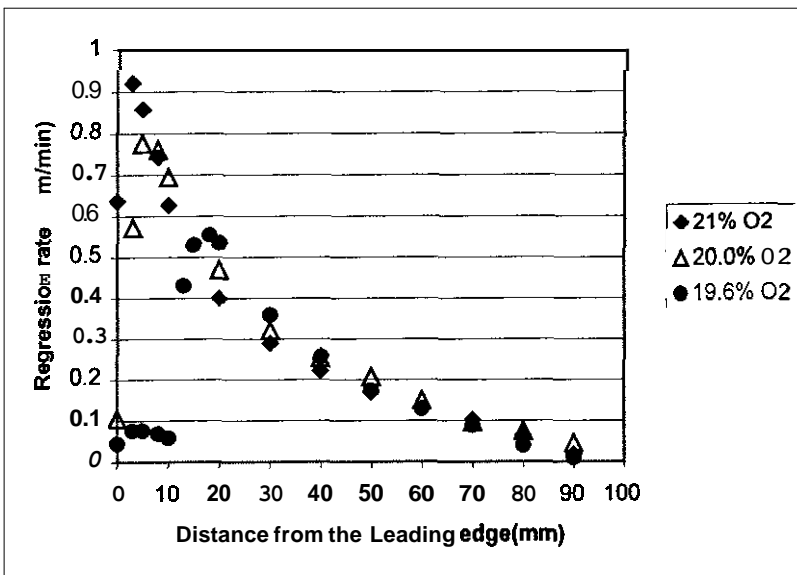


Figure 5. Effects of oxygen dilution on the sample burning rate.

This is because with oxygen dilution the flame initially attached downstream from the leading edge to balance the flow time and reaction time and maintain the value of the critical Damkohler number. This shift in attachment location is the quenching distance. It was visually estimated that the quenching distance was about 5 and 15 mm in the tests with 20 and 19.6% O₂, respectively. However, during the 5 min of the test, the flame spread slowly toward the leading edge decreasing the quenching distance. Kodama et al. [12] measured a quenching distance of 15 mm in a test with heptane with inlet velocity of 103 cm/s and 19.5% oxygen concentration. They also reported that the flame was extinguished for oxygen concentrations below 18%. Figure 5 shows that the sample regression rate decreases with a decrease in oxygen concentration especially in the leading section of the sample. This occurs as a result of the flame attaching further downstream and also of the lower heat feedback to the surface, as discussed in the previous section. It has been shown theoretically [13,14] that in a forced flow boundary layer flame, a much higher percentage of the heat is generated in the leading section of the plate (or sample) and therefore, chemistry is very important in this section. The effects of oxygen dilution would reduce the chemical reaction rates and result in reduced heat generation rate. It can also result in higher sensible heat absorption because of the additional nitrogen. The latter effect is expected to be small in these tests since the

additional nitrogen was about 5 or 7% of the total volume flow. Both effects would, however, affect heat feedback to the sample surface and hence surface regression rate.

The mass flux at any X location **can** be obtained from the regression rate and **PMMA** density. Figure 6 shows the percent of mass burned up to a streamwise location vs the normalized distance from the leading edge, for three tests with 21, 20, and 19.6% O₂ concentration. This percentage is the ratio of the sum of the sample mass lost up to that location divided by the total mass lost in the entire length of the sample during the test. The base case results show that most burning takes place in the leading section as a result of the non-uniform heat feedback inherent in boundary layer diffusion flames; e.g., during the 5 min burn and with a U=84 cm/s, about 85% of the mass loss occurred in the first 50% of sample length and nearly 40% of the mass loss took place in the leading 10% of the sample length. This implies that a boundary layer flame would be suppressed more effectively by delivering the suppressant near the leading edge, where most of the burning takes place rather than downstream. The difference between the base case data and the data with oxygen dilution can be explained by the increased quenching distance; e.g., with the base case test, the flame attached at the leading edge and the first 10 mm experienced high heat feedback and high burning rate. However, with the 19.6% oxygen the first 10 mm of the sample had no flame over it and the burning rate was zero. The small mass loss was recorded during sample ignition when the entire surface was irradiated.

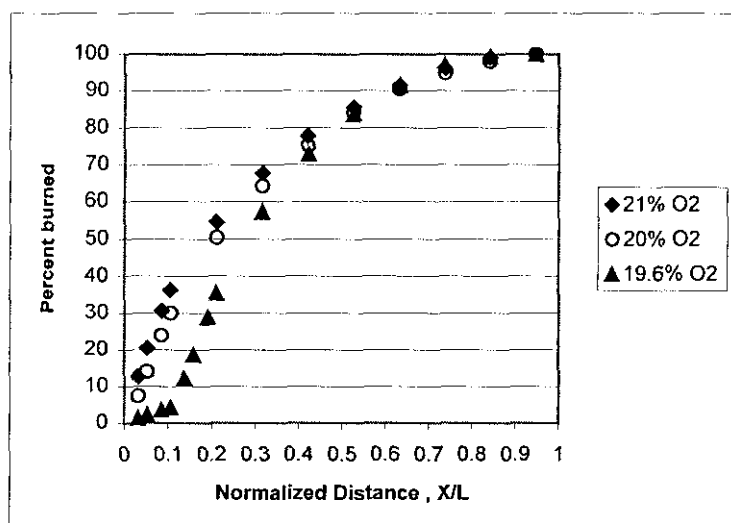


Figure 6. Contribution of the various sections of the sample to the total burning rate in tests with varying oxygen concentration.

CONCLUDING REMARKS

This paper presented the preliminary results in the study of water mist suppression mechanisms in boundary layer diffusion flames. It discussed the characterization of the base case flame in preparation for the addition of fine water mist. **Also**, the results of tests to study only the oxygen dilution effects, where oxygen concentration in the oxidizer air was diluted with up to 7% additional nitrogen were presented. The results can be summarized as follows:

1. Sample burning rate decreases sharply with stream-wise distance from the leading edge as a result of higher rate of heat feedback in the leading section. A disproportionately higher burning rate is measured in the leading section and therefore, it would be desirable to deliver most of the mist in this section for optimum effectiveness.
2. Temperature profiles in the gas phase show a higher gradient in the leading section, which is consistent with the higher burning rate measured in this section.
3. The dilution of oxygen in oxidizer air affects the flame stability by increasing the quenching distance. The quenching distance with 19.6% oxygen, under our experimental conditions, was about 15 mm.

4. The corresponding peak flame temperatures decreased with oxygen dilution, with **19.6%** oxygen, the maximum flame temperature decreased by about **150 K**. This is due to the decrease in heat generation rate especially in the leading section of the flame where chemistry is important.

ACKNOWLEDGMENTS

The work was funded by the Office of Naval Research, Code **334**, under the Damage Control Task of the FY01 Surface Ship Hull, Mechanical and Electrical Technology Program (**PE060212IN**).

REFERENCES

1. Rashbash, D.J., Rogowski, Z.W., and Stark, G.W.V., "Mechanism of Extinction of Liquid Fires with Water Sprays," *Combust. Flame*, **4**, pp. **223-234**, **1960**.
2. Braidech, N.M., Neale, J.A., Matson A.F., and Dufour, R.E., "The Mechanism of Extinguishments of Fire by Finely Divided Water," Underwriters Laboratory, Inc., for the National Board of Fire Underwriters, New York, pp. **73**, **1955**.
3. Rashbash, D.J., "The Extinction of Fire with Plain Water: A Review," *Fire Safety Science – Proceeding of the First International Symposium Hampshire*, pp. **1145-1163**, **1986**.
4. Ndubizu, C.C., Ananth, R., and Tatem, P.A., "On Water Mist Fire Suppression Mechanisms in a Gaseous Diffusion Flame," *Fire Safety J.*, **31**, pp. **253-276**, **1998**.
5. Seshadri K., "Structure and Extinction of Laminar Diffusion Flames Above Condensed Fuels with Water and Nitrogen," *Combust. Flame* **33**, pp. **197-215**, **1978**.
6. Lentati, A.M., and Chelliah, H.K., "The Dynamics of Water Droplets in a Counter Flow Field and its Effects on Flame Extinction," *Proceeding of the Fall Technical Meeting, The Eastern states Section of the Combustion Institute*, Hilton Head, SC, p. **281**, **1996**.
7. Ndubizu, C.C., Ananth, R., and Tatem, P.A., "Experimental Investigation of a Forced Flow Boundary Layer Flame Over PMMA," 2nd Joint meeting of the U.S Sections of the Combustion Institute Oakland C.A, Paper no. **58,2001**.
8. Holve, D.J., and Sawyer, R.F., "Diffusion Controlled Combustion of Polymers," *Fifteenth Symposium (International) on Combustion*, The Combustion Institute, pp. **351-361**, **1974**.
9. Mekki, K., Atreya, A., Agrawal, S., and Wichman, I., "Wind-Aided Flame Spread Over Charring and Non-Charring Solids, and Experimental Investigation," *Twenty-third Symposium (International) on Combustion*, The Combustion Institute, pp. **1701-1707**, **1990**.
10. Seshadri, K., and Williams, F.A., "Structure and Extinction of Counterflow Diffusion Flames Above Condensed Fuels: Comparison Between Poly(Methyl Methacrylate) and its Liquid Monomer Both Burning in Nitrogen-Air Mixtures," *J. Polymer Sci: Polymer Chemistry Edition*, **16**, pp. **1755-1778**, **1978**.
11. Williams, F.A., "*Combustion theory*" Addison-Wesley Publishing Co., Reading, MA, p. **495**, **1985**.
12. Kodama, H., Miyasaka, K., and Fernandez-Pello, A.C., "Extinction and Stabilization of a Diffusion Flame on a Flat Combustible Surface with Emphasis on the Thermal Controlling Mechanisms," *Combust. Sci. and Tech*, **54**, pp. **37-50**, **1987**.
13. Ananth, R., Ndubizu, C.C., Tatem, P.A., Patnaik, R., and Kailasanath, K., "Boundary Layer Diffusion Flame Over a Porous Plate," 2nd Joint meeting of the US Sections of the Combustion Institute, Oakland, C.A, Paper no. **56,2001**.
14. Chien, C.H., and Tien, J.S., "Diffusion Flame Stabilization at the Leading Edge of a Fuel Plate," *Combust. Sci. and Tech.*, **50**, pp. **283-306**, **1986**.